

Nonlinear Dust Acoustic Waves, Shocks and Stationary Structures in a DC Glow Discharge Dusty Plasma

Robert L. Merlino, Jonathon R. Heinrich and Su-Hyun Kim

Department of Physics and Astronomy, The University of Iowa, Iowa City, IA 52242 USA

Abstract. The dust acoustic wave (DAW) is a very low frequency (tens of Hz) dust density wave in which the dust particles participate in the wave dynamics. The early experimental observations of DAWs showed that the wave was self-excited by a modest relative ion drift and grew to very high amplitudes ($\sim 100\%$). In the first part of this paper we describe experiments showing the self-steepening of nonlinear DAWs into dust acoustic shock waves. In the second part we present observations of self-organized, stationary (i.e., non-propagating), stable, dust density structures formed in a DC glow discharge dusty plasma.

Keywords: Dusty plasma, dust acoustic shocks, structure formation

PACS: 52.27, 43.25.+y, 47.54.De

INTRODUCTION

Dust acoustic wave (DAW) was the term first used by Rao, Shukla, and Yu [1] in 1990 to describe the low frequency wave in a dusty plasma in which the dust particles (hereafter, microparticles) participate in the wave dynamics. Since the phase speed of the DAW is well below the electron and ion thermal speeds, both the electrons and ions were taken to be in Boltzmann equilibrium, and the dispersion relation was obtained by linearizing the continuity and momentum equations for the dust. In the long-wavelength acoustic limit, where the wave frequency, $\omega \ll \omega_{pd}$, where ω_{pd} is the dust plasma frequency, the dispersion relation is $(\omega/k)^2 = V_{Td}^2 + \omega_{pd}^2 \lambda_D^2$, where k is the wavenumber, λ_D is the plasma Debye length defined by, $\lambda_D^{-2} = \lambda_{De}^{-2} + \lambda_{Di}^{-2}$, where λ_{De} and λ_{Di} are the electron and ion Debye lengths, and $V_{Td} = \sqrt{k_B T_d / m_d}$, is the dust thermal speed, with T_d and m_d , the dust temperature and mass.

A remarkable aspect of reference [1] was that the authors derived not only the linear theory of the DAW, but they also obtained a generalized K-dV equation to analyze nonlinear DAWs, seemingly anticipating the fact that the DAW waves observed in the laboratory a few years later were of large amplitude ($\tilde{n}_d/n_d \sim 1$) [2].

As discussed by Morfill et al., [3], dusty plasmas can be operated essentially as one-component plasmas when the interactions between the microparticles dominate over the interactions between the microparticles and background neutral gas atoms. This enables the use of a dusty plasma as a surrogate system in which to study the

behavior of fluids, e.g., shock wave physics. Microparticles can be studied at the kinetic level, which is not possible in ordinary fluids. To illustrate this connection between single phase dusty plasmas and fluids, we consider the following one-dimensional model of a dusty plasma in which the microparticles are described by the fluid equations with the plasma electrons and ions mediating the electrostatic interactions between the particles and providing the shielding.

Let m , n , u , and q represent respectively, the dust mass, density, fluid velocity and magnitude of the dust charge which is taken to be negative, $\rho_m = mn$, the dust mass density and $\rho_q = qn$, the dust charge density. The dust dynamics can be described by the continuity and the momentum equations,

$$\frac{\partial \rho_m}{\partial t} + \frac{\partial(\rho_m u)}{\partial x} = 0, \quad \rho_m \left(\frac{\partial u}{\partial t} + u \frac{\partial u}{\partial x} \right) = \rho_q \frac{\partial \varphi}{\partial x} - \frac{\partial p}{\partial x} + \eta \frac{\partial^2 u}{\partial x^2}, \quad (1a,b)$$

where φ is the electrostatic potential, p is the dust pressure, and η is the dust viscosity. For potentials which vary on time scales well below the dust plasma frequency, the ions and electrons can be described by, $0 = \mp \rho_j \partial \varphi / \partial x - \partial p_j / \partial x$, where $\rho_j = en_j$, is the charge density, and p_j is the pressure, with the subscript, $j = i, e$, denoting ions and electrons. Using charge neutrality, $\rho_i = \rho_e + \rho_q$, and the Boltzmann relations, the electric potential can be expressed in terms of the plasma pressure, $\rho_q \partial \varphi / \partial x = -\partial(p_i + p_e) / \partial x$, so that equation (1b) can be written in the form

$$\rho_m \left(\frac{\partial u}{\partial t} + u \frac{\partial u}{\partial x} \right) = -\frac{\partial P}{\partial x} + \eta \frac{\partial^2 u}{\partial x^2}, \quad (2)$$

where, $P = p + p_i + p_e$. Eq. (2) is the Navier-Stokes equation of fluid dynamics, thus showing the similarity between a single phase dusty plasma and ordinary fluids.

This paper describes two investigations: (i) steepening of nonlinear DAWs and DA shockwaves (DASW), and (ii) the formation of stationary (non-propagating) stable dust density structures, similar to those predicted by Tsytovich and Morfill [4,5].

NONLINEAR DUST ACOUSTIC WAVES AND SHOCKS

If the dust continuity and momentum equations are linearized, and viscosity neglected, the solutions representing small amplitude waves have the functional form $f(x - ct)$, where c is the wave phase speed as found in [1]. However, for nonlinear waves, it is well-known [6] that for an inviscid fluid, the resulting Euler equation admits self-steepening shock solutions. In this case u and ρ_m now have functional forms $f[x - (c + u)t]$, so that the wave speed depends on the wave amplitude, leading to nonlinear wave steepening.

The observations of DASW were performed in a DC glow discharge dusty plasma in argon gas at a pressure of 100 mtorr using kaolin dust in $\approx 1 \mu\text{m}$ size range. An

electrically floating slit was used in front of the anode to produce an electric potential configuration that favored the formation of high compression dust structures that evolved into shocks. The schematic diagram of the setup and single frame video image of the nonlinear DASWs is shown in Fig. 1(a). The electric potential configuration created by the slit enhanced the dust density perturbation which then evolved into a series of shocks that propagated in the direction away from the anode. The scattered light intensity, which is proportional to the dust density is shown in Fig. 1(b).

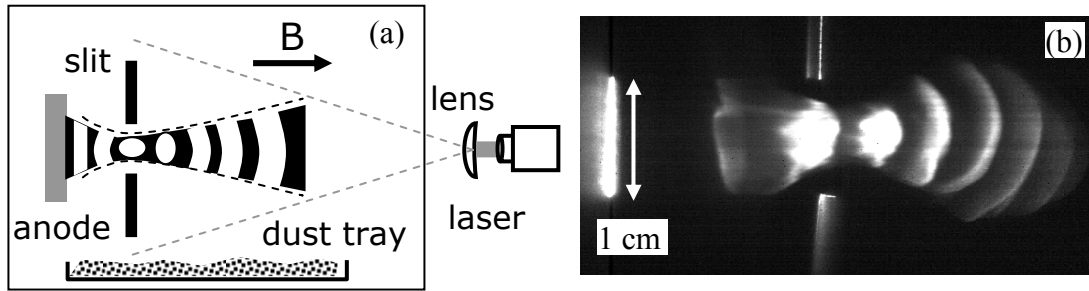


FIGURE 1. (a) Schematic diagram of the experimental setup used to produce DASWs. The slit is placed in front of the anode to produce a nozzle-like configuration that is conducive to the formation of shocks. (b) Single frame image of DASWs travelling away from the anode, produced using a thin sheet of 532 nm laser light to illuminate the dust particles which are then imaged with a CMOS video camera.

The time evolution of a typical shock wave is shown in Fig. 2. These profiles were obtained from single frame video images taken at 500 fps. The shocks developed into sawtooth-like structures and steepened as they travelled. The peak value of each profile was normalized to the peak at $t = 0$ (an arbitrarily chosen initial observation time). The dashed line shows how the shock amplitude decreased in time. Further details of the DASW experiments can be found in [7]. The observed DASWs were similar to those in the numerical calculations of Eliasson and Shukla [8], which did not include dissipation or dispersion which would limit the shock thickness.

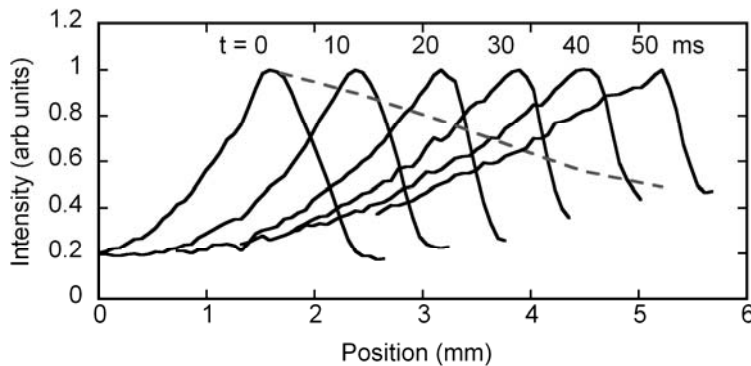


FIGURE 2. Scattered light intensities (\sim dust density) of the DASW at 10 ms intervals. Profiles were normalized to the peak value at $t = 0$; actual peak values are shown as the dashed line.

A plot of the position, amplitude and thickness of the shock vs. time is shown in Fig. 3. The shock speed is ≈ 75 mm/s, with a Mach number $M \sim 1$. The shock

thickness decreased in time and stabilized to a value $\delta \approx 0.3$ mm, which was less than that expected from dust-neutral collisions. Several mechanisms have been proposed to account for the dissipation necessary to form a stationary shock. These include strong correlations between dust particles and non-adiabatic dust charge variations [9-11]. For the shocks that we have observed, the minimum thickness was on the order of the interparticle spacing, $\Delta \sim n_d^{-1/3}$.

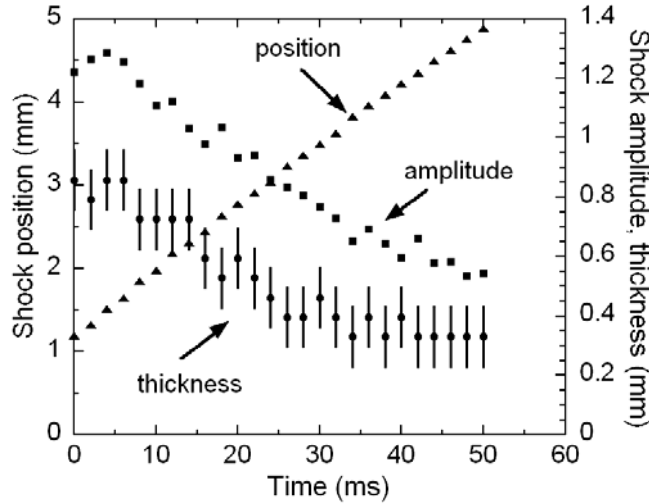


FIGURE 3. Shock position, amplitude and thickness vs. time.

OBSERVATION OF STATIONARY DUST STRUCTURES

Due to the flux of plasma on the dust particles, an ionization source is needed to maintain a dusty plasma. Thus, dusty plasmas are inherently open systems which are subject to self-organized structurization. This process was studied theoretically by Morfill and Tsytoich [5] who showed that a homogeneous dusty plasma is unstable to the formation of multiple dust clumps separated by dust voids. The mechanisms involved in this process are ionization and ion drag which are responsible for the formation of voids. D'Angelo [12] analyzed theoretically the ionization instability in a dusty plasma including the effects of ion drag. He showed that when the ion drag frequency was above a critical value, a zero-frequency (non-propagating) dust density perturbation would grow.

We have observed the formation of stationary (non-propagating), stable dust density structures in a DC glow discharge dusty plasma. The parameter controlling the transformation to stationary structures in the discharge was the discharge current, which controls the plasma density (plasma density increases with discharge current). For discharge currents in the range of a few mA to 10 mA, we observed spontaneously excited, propagating dust acoustic waves due to the ion-dust streaming instability [13]. When the discharge current was increased to ~ 15 mA, the dust suspension transformed into an alternating pattern of high and low dust density (partial voids), as shown in Fig. 4(a). In three-dimensions, the dust was arranged in nested conical-like

structures. To illustrate the robustness of these structures, we show in Fig. 4(b) profiles of the light intensity (proportional to dust density) across the region shown as the dashed line in Fig. 4(a). Ten overlapping profiles are shown, which were taken every 100 frames over a 1000 frame video segment at 30 fps. The structurization was observed in dusty plasmas using glass microspheres, spherical iron and copper particles, and kaolin powder.

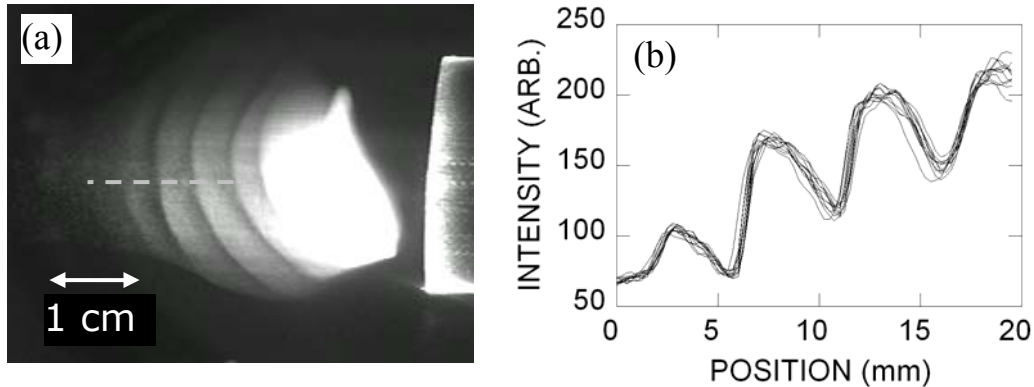


FIGURE 4. (a) Single frame video image of a stationary dust density structure. The bright regions are regions of high dust density which are separated by thin partial dust voids. (b) Profiles of the light intensity over the line in (a) taken over a 1000 frame interval at 30 fps. data taken with spherical micron size iron dust particles. The rectangular object on the right is the anode.

A three-dimensional view of the structure, which was constructed from multiple video images obtained by moving the illuminating laser sheet to multiple locations in the dust cloud, is shown in Fig. 5.

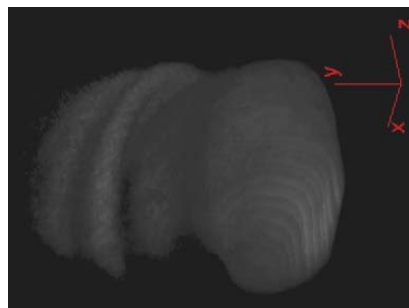


FIGURE 5. A 3-D perspective view of the dust structure. The anode (not shown) is to the right.

The wavelength of the structures was in the range of 3 - 6 mm and decreased with increasing discharge current (plasma density) as shown in Fig. 6. The decrease in wavelength with increasing plasma density is in qualitative agreement with the theory of Morfill and Tsytoich [4] who showed that the maximum growth rate corresponds to a wavenumber, $k \approx a / \lambda_{Di}^2$ where λ_{Di} is the ion Debye length and a is the dust size,

so that the structure wavelength, Λ , is given by, $\Lambda = 2\pi\lambda_{Di}^2 / a$, which scales with ion density, n_i , as $\Lambda \sim n_i^{-1} \sim I_D^{-1}$, where I_D is the discharge current.

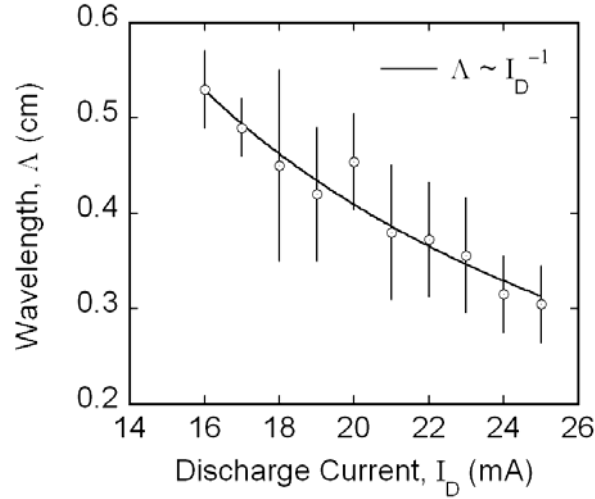


FIGURE 6. Dependence of the structure wavelength on discharge current.

Self-organized dust structure formation is of great interest for processes in interstellar molecular clouds, protostars, planet formation and planetary rings.

ACKNOWLEDGMENTS

This work was supported by The Department of Energy and National Science Foundation. We would like to thank V. N. Tsytovich and S. A. Khrapak for useful communications.

REFERENCES

1. N. N. Rao, P. K. Shukla, and M. Y. Yu, *Planet. Space Sci.* **38**, 543-546 (1990).
2. A. Barkan, R. L. Merlino, and N. D'Angelo, *Phys Plasmas* **2**, 3563-3566 (1995).
3. G. E. Morfill, S. A. Khrapak, A. V. Ivlev, B. A. Klumov, M. Rubin-Zuzic, and H. M. Thomas, *Phys. Scripta* **T107**, 59-64 (2004).
4. V. N. Tsytovich, *Au. J. Phys.* **51**, 763-834 (1998).
5. G. Morfill and V. N. Tsytovich, *Plasma Phys. Reports* **26**, 682-690 (2000).
6. see, e.g., L. D. Landau and E. M. Lifshitz, *Fluid Mechanics*, Reading: Addison Wesley Publishing Co. Inc., 1959, pp. 366-370; D. Montgomery, *Phys. Rev. Lett.* **103**, 1465-66 (1967).
7. J. Heinrich, S.-H. Kim, and R. L. Merlino, *Phys. Rev. Lett.* **103**, 115002 (2009).
8. B. Eliasson and P. K. Shukla, *Phys. Rev. E* **69**, 067401 (2004).
9. M. R. Gupta, S. Sarkar, S. Ghosh, M. Debnath, and M. Khan, *Phys. Rev. E* **63**, 046406 (2001).
10. A. A. Mamun and R. A. Cairns, *Phys. Rev. E* **79**, 055401 (2009).
11. H. Asgari, S. V. Muniandy, and C. S. Wong, *Phys. Plasmas* **18**, 013702 (2011).
12. N. D'Angelo, *Phys. Plasmas* **5**, 3155-3160 (1998).
13. R. L. Merlino, *Phys. Plasmas* **16**, 124501 (2009).